



HHS Public Access

Author manuscript

Ann Thorac Surg. Author manuscript; available in PMC 2017 May 01.

Published in final edited form as:

Ann Thorac Surg. 2016 May ; 101(5): 1958–1962. doi:10.1016/j.athoracsur.2015.12.075.

FROM 3D PRINTING TO 5D PRINTING: ENHANCING THORACIC SURGICAL PLANNING AND RESECTION OF COMPLEX TUMORS

Erin A Gillaspie, MD¹, Jane S Matsumoto, MD², Natalie E Morris¹, Robert J Downey, MD³, K Robert Shen, MD¹, Mark S Allen, MD¹, and Shanda H Blackmon, MD¹

¹Division of Thoracic Surgery, Mayo Clinic, Rochester MN

²Division of Radiology, Mayo Clinic, Rochester MN

³Thoracic Service, Department of Surgery, Memorial Sloan Kettering Cancer Center, NY, NY

Abstract

Purpose—Three dimensional (3D) printing of anatomic models for complex surgical cases improves patient and resident education, operative team planning, and guides surgery. Our group intends to describe two additional dimensions.

Description—The process of 5-dimensional printing was developed for surgical planning. Pretreatment computed tomography and positron emission tomography scans were reformatted and fused. Selected anatomy from these studies along with post treatment computed tomography and magnetic resonance images were co-registered and segmented. This fused anatomy was converted into stereolithography files for 3D printing.

Evaluation—A patient presenting with a complex thoracic tumor was selected for 5-dimensional printing. 3D and 5-dimensional models were prepared to allow surgical teams to directly evaluate and compare the added benefits of information provided by printing in 5 dimensions.

Conclusions—Printing 5-dimensional models in patients with complex thoracic pathology facilitates surgical planning, selecting margins for resection, anticipating potential difficulties, teaching for learners, and education for patients.

Corresponding Author: Shanda H. Blackmon, M.D., M.P.H., FACS, Associate Professor, Division of General Thoracic Surgery, Mayo Clinic, 200 First St, SW, Rochester, MN 55905, blackmon.shanda@mayo.edu, Tel: (507) 284-8462.

Disclaimer

The Society of Thoracic Surgeons, the Southern Thoracic Surgical Association, and *The Annals of Thoracic Surgery* neither endorse nor discourage the use of the new technology described in this article.

Disclosure and Freedom of Investigation Statement

The funds used to perform the testing are provided by an internal grant through Mayo Clinic. The technology was purchased by the institution for the purposes of 3D printing and no additional purchases were necessary, rather a new application for the technology was developed. Authors had full control of the design of the study, methods, outcome parameters, analysis of data and the creation of the manuscript. The patient was not billed for the printing of the models, and the institution has independently funded this research to explore possibilities that exist with complex imaging.

Publisher's Disclaimer: This is a PDF file of an unedited manuscript that has been accepted for publication. As a service to our customers we are providing this early version of the manuscript. The manuscript will undergo copyediting, typesetting, and review of the resulting proof before it is published in its final form. Please note that during the production process errors may be discovered which could affect the content, and all legal disclaimers that apply to the journal pertain.

Keywords

lung cancer; lung; chest wall; imaging (3D anatomic models); thoracic surgery; operations New Technology

Technology

In 1982, Hideo Kodama from the Nagoya Municipal Industrial Research Institute provided the first description of 3D (three-dimensional) printing. Ten years later, the first 3D printer was developed. While initially used in manufacturing, it has been adapted for medical applications. In planning surgical procedures, a 3D model conveys key anatomical relationships to surgeons in a way that 2D (two-dimensional) images on a computer currently do not.¹⁻⁹ In addition to surgical planning, 3D printing technology has also been used to create patient-specific implantable scaffolds for biological grafts.¹⁰⁻¹¹

For surgeons, the 3D model proves particularly helpful in patients who have a complex operative history, when there is an intricate relationship of tumor to surrounding structures, and when planning a multi-disciplinary team approach.¹⁻⁹ Extending the technology, a collaborative team of surgeons and radiologists at the Mayo Clinic in Rochester, MN, have now created models incorporating five dimensions. 5D (five-dimensional) printing incorporates data utilized to create 3D models, and, in addition, incorporates data regarding tumor response and physiologic activity to induction therapy. The dimensions of 5D printing are then: height (y axis), width (x axis), depth (z axis), change in tumor size (change in CT measured dimensions), and physiology (change in PET measured FDG avidity).

In this report, we describe the application of this 5D printing technique to the preoperative planning of complex thoracic surgical oncologic cases.

Technique

Patient Preparation & Image Acquisition

In the case described, prior to initiating therapy, high resolution chest computerized axial tomography (CT) scan (1.5–3.0mm) with intravenous contrast and 18F-fluorodeoxyglucose positron emission tomography (PET) were performed. After completion of induction chemotherapy, a CT chest with IV contrast, magnetic resonance imaging (MRI) of the brachial plexus and PET imaging were performed.

Image Segmentation, Processing and 3D to 5D Printing

A 5D anatomic model was printed using sequenced imaging data from the patient's CT, MRI, and PET scans. The PET scan was re-oriented with rigid 3 point reformat and then merged with the CT images. The DICOM (Digital Imaging and Communication in Medicine) imaging data from these studies, along with the brachial plexus MR, was imported into proprietary software (Materialise, Belgium). The desired anatomy is selected using both automated and hand segmenting tools. The selected anatomy included the aorta, pulmonary arteries and veins, SVC, upper ribs, sternum, spine, brachial plexus, and upper

thoracic nerve roots. Pre-treatment and post-treatment CT and PET images were also segmented. 5D anatomic models incorporated pre-treatment and post-treatment CT and PET images to create a combined image displaying the tumor prior to treatment, and the post-treatment residual tumor, color-coding for FDG activity. The segmented data were converted into a virtual 3D anatomic model (Figure 1) which is then exported into an STL (Stereolithography) file format. As a quality check, the final STL file was reimported into the source imaging data to ensure that the outline accurately matched the original images.

The STL files were exported to the 3D printer software for selection of materials, both rigid and flexible, and various colors for the anatomic structures. The original tumor was assigned a clear material and the post-treatment tumor was assigned a solid color to allow visible representation of tumor shrinkage. Life-sized models were then printed on a polyjet 3D printer which uses liquid photopolymers cured with UV light (Stratasys Inc., Eden Prairie, MN.). The model is printed with surrounding support material which helps it hold shape until the polymer fully hardens (Figure 2). It is then washed-off with pressurized water. The life-sized anatomic models (Figures 3a & 3b) are then cleaned and prepared. The transparent portion of the model with the embedded residual tumor is printed separately and is polished and coated with a clear coat material to promote visualization of the tumor within (Figure 3b). These nodal and tumor areas are then assembled into the model.

Clinical Experience

A 39 year-old-woman, who presented with chest pain, was found to have a left superior sulcus tumor (Figure 4a) with a suspicious aortopulmonary (AP) window lymph node. She underwent neoadjuvant chemoradiotherapy with cisplatin, etoposide and 60 Gy of radiation at an outside facility without biopsy of the lymph node. Restaging imaging revealed a marked reduction in the size of the tumor (Figure 4b) and lymph node, but persistent invasion into the left subclavian artery, first rib, T2–T3 nerve roots, and T2–3 vertebral bodies. A cerebral angiogram confirmed widely patent innominate, carotid and vertebral arteries with a complete Circle of Willis.

A 5D model was printed and used to guide initial operative planning (Figures 3a & 3b). The vascular, orthopedic and thoracic teams met pre-operatively to discuss and rehearse the surgical procedure.

A mediastinoscopy and left video-assisted thoracoscopy were performed to sample mediastinal lymph nodes, which were found to be pathologically benign. The team proceeded with an osteotomy of the posterior aspect of the left first through third ribs, rhizotomy of T1–T3 nerve roots and a T2–T3 hemi-vertebrectomy from a posterior approach (Figure 5). Two days later a left trapdoor incision allowed the team to perform the resection. This included a left upper lobectomy, completion anterior chest wall resection (removing the areas delineated by the 5D model as “prior tumor” or “remaining FDG-avid” rather than visible tumor at the time of resection) with partial subclavian artery resection and left carotid-subclavian bypass (Figure 6). The specimen was removed en bloc (Figure 7) and the model was used to orient the pathology team for processing. A pericardial fat pad and thymic fat pad flap were used for bronchial stump re-enforcement and to interpose between

the carotid-subclavian bypass graft and the vein. The chest wall was reconstructed with biomesh and covered with a pectoralis advancement flap. Pathologic examination demonstrated an R0 resection containing adenocarcinoma with <10% viable tumor, pathologic stage T1aN0M0.

The postoperative course was significant for pneumonia which required antibiotic therapy alone. The patient ultimately was discharged home on postoperative day 20 in stable condition without limitations.

At the 4 month evaluation, physical examination revealed a good range of motion in both of her arms, with equal strength and sensation throughout. She did have a mild Horner's Syndrome on the left, as expected. The CT scan demonstrated no evidence of recurrent disease. No additional chemotherapy was administered.

Comment

In complex thoracic surgical cases, distorted anatomy from tumor growth and invasion of surrounding structures, along with changes that occur with neoadjuvant treatment, are factors that complicate surgical planning. 5D printing allows creation of a tangible representation of the effectiveness of treatment and residual activity discovered on FDG-PET imaging, specifically two clear benefits. First, utilizing the guide of remaining FDG activity and prior tumor location can potentially enhance the R0 resection rate. Second, allowing the team to spare parts of structures that were never clinically involved but may appear abnormal from prior radiation at the time of resection. We have utilized 3D printed models to overcome some of the complex issues related to surgical planning, however, the addition of a 5D model integrates additional data in a way that everyone from the patient to the surgeon can readily interpret.

In the case presented, the 5D model enabled resection of any areas of previous tumor involvement and avoidance of resection of structures that clearly do not appear to be involved, potentially enhancing the probability of an R0 resection. This model aims to enhance details available to the team to help guarantee adequate resection every case.²⁻¹⁴ Many studies have confirmed the benefit of R0 Pancoast tumor resection.¹²⁻¹⁴ In our experience, the team reported ease of planning, enhanced guidance during surgery, and superior intra-operative communication with multiple members of the operating team and pathology specimen orientation. Unfortunately, this process is not currently reimbursed, and most centers are internally funding this to enhance their team's ability to communicate and plan complex surgery. Printers typically start at \$150,000 and each structure will depend on the amortized cost of the printer, the time for radiologists and surgeons to select and segment the imaging, plus the material, which for Pancoast tumors is around \$1500 (taking about 50 hours to print). In the future, other aspects of surgical anatomy, physiology, and change over time may be added as additional dimensions of information to be incorporated and printed, again enhancing the assimilation of complex data used for surgical and oncologic planning.

References

1. Tam MD, Latham T, Brown JR, Jakeways M. Use of a 3D Printed Hollow Aortic Model to Assist EVAR Planning in a Case with Complex Neck Anatomy: Potential of 3D Printing to Improve Patient Outcome. *J Endovasc Ther*. 2014 Oct; 21(5):760–2. [PubMed: 25290807]
2. Igami T, Nakamura Y, Hirose T, Ebata T, Yokoyama Y, Sugawara G, Mizuno T, Mori K, Nagino M. Application of a three-dimensional print of a liver in hepatectomy for small tumors invisible by intraoperative ultrasonography: Preliminary experience. *World J Surg*. 2014 Dec; 38(12):3163–6. [PubMed: 25145821]
3. Chung KJ, Hong do Y, Kim YT, Yang I, Park YW, Kim HN. Preshaping Plates for Minimally Invasive Fixation of Calcaneal Fractures Using a Real-Size 3D-Printed Model as a Preoperative and Intraoperative Tool. *Foot Ankle Int*. 2014 Nov; 35(11):1231–6. [PubMed: 25053782]
4. Chae MP, Lin F, Spychal RT, Hunter-Smith DJ, Rozen WM. 3D-Printed haptic “Reverse” models for preoperative planning in soft tissue reconstruction: A case report. *Microsurgery*. 2014 Jul 21.
5. Nakada T, Akiba T, Inagaki T, Morikawa T. Thoracoscopic anatomical subsegmentectomy of the right S2b + S3 using a 3D printing model with rapid prototyping. *Interact Cardiovasc Thorac Surg*. 2014 Jul 6.
6. Zopf DA, Mitsak AG, Flanagan CL, Wheeler M, Green GE, Hollister SJ. Computer Aided-Designed, 3-Dimensionally Printed Porous Tissue Bioscaffolds for Craniofacial Soft Tissue Reconstruction. *Otolaryngol Head*.
7. Carrel JP, Wiskott A, Moussa M, Rieder P, Scherrer S, Durual S. 3D printed TCP/HA structure as a new osteoconductive scaffold for vertical bone augmentation. *Clin Oral Implants Res*. 2014 Oct 28.
8. Chang JW, Park SA, Park JK, Choi JW, Kim YS, Shin YS, Kim CH. Tissue-engineered tracheal reconstruction using three-dimensionally printed artificial tracheal graft: preliminary report. *Artif Organs*. 2014 Jun; 38(6):E95–E105. [PubMed: 24750044]
9. Blackmon SH, Gillaspie E, Arun J, Dickinson K, Rose P. Minimally Invasive Approach to Pancoast Tumor using 3D Printing. *Annals of Thoracic Surgery*. 2015 Aug; 100(2):692–7. Jan 20. DOI: 10.1016/j.athoracsur.2015.03.115 [PubMed: 26234839]
10. Seol YJ, Kang HW, Lee SJ, Atala A, Yoo JJ. Bioprinting technology and its applications. *Eur J Cardiothorac Surg*. 2014 Sep; 46(3):342–8. [PubMed: 25061217]
11. Fishman JM, Wiles K, Lowdell MW, De Coppi P, Elliott MJ, Atala A, Birchall MA. Airway tissue engineering: an update. *Expert Opin Biol Ther*. 2014 Oct; 14(10):1477–91. [PubMed: 25102044]
12. Rusch VW, Parekh K, Leon I, et al. Factors determining outcome after surgical resection of T3 and T4 lung cancers of the superior sulcus. *J Thorac Cardiovasc Surg*. 2000; 119:1147–53. [PubMed: 10838531]
13. Deslauriers J, Tronc F, Fortin D. Management of tumors involving the chest wall including Pancoast Tumors and tumors invading the spine. *Thorac Surg Clin*. 2013; 23:313–325. [PubMed: 23931015]
14. Kozower BD, Larnar JM, Dettlerbeck F, et al. Special treatment issues in non-small cell lung cancer. *Chest*. 2013; 143(5 suppl):e369s–e399s. [PubMed: 23649447]

The field of 3D printing involves multiple specialists like engineers, doctors, and educators working together to create models for surgical planning. Incorporating information about the degree of tumor response to therapy over time (4th dimension) and physiologic activity (5th dimension), into the model enhances its utility. This manuscript describes the process of creating a five dimensional printed model.

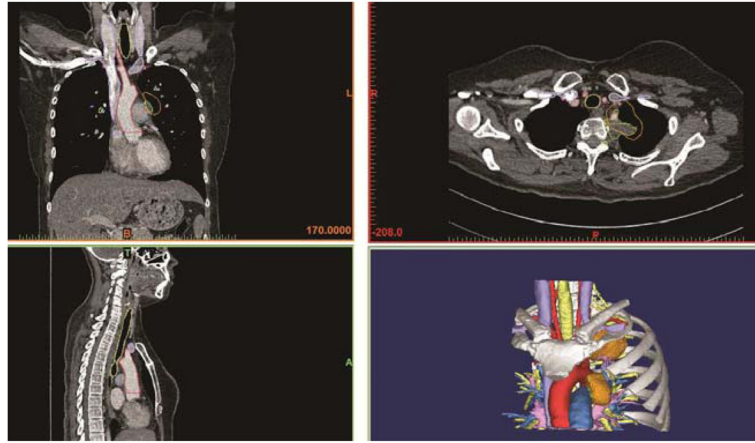


Figure 1. The CT scans are used to segment the image, which is then converted into a 3D anatomic model. The bottom right image represents the final segmentation.

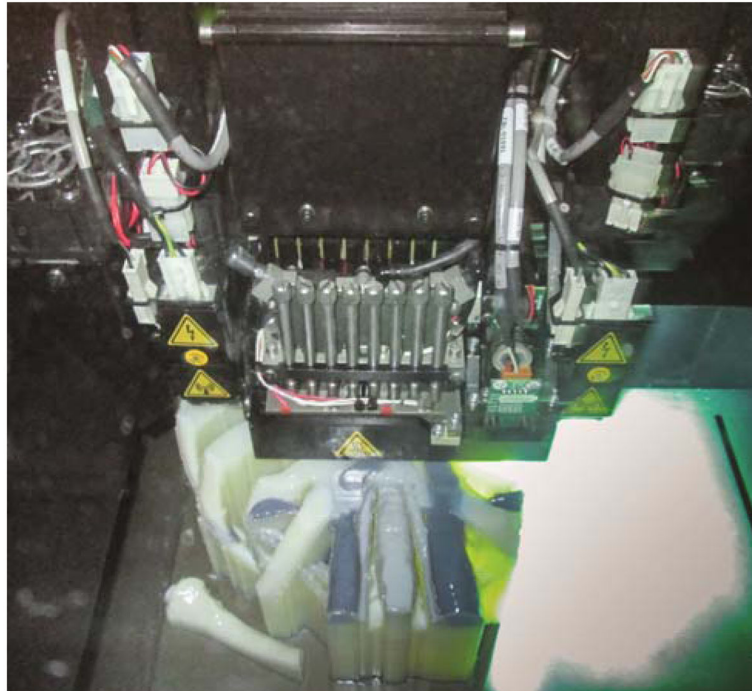


Figure 2. The printer is in the process of printing the model, laying down material in a thin layer and then exposing it to UV light to harden before the next layer is applied.



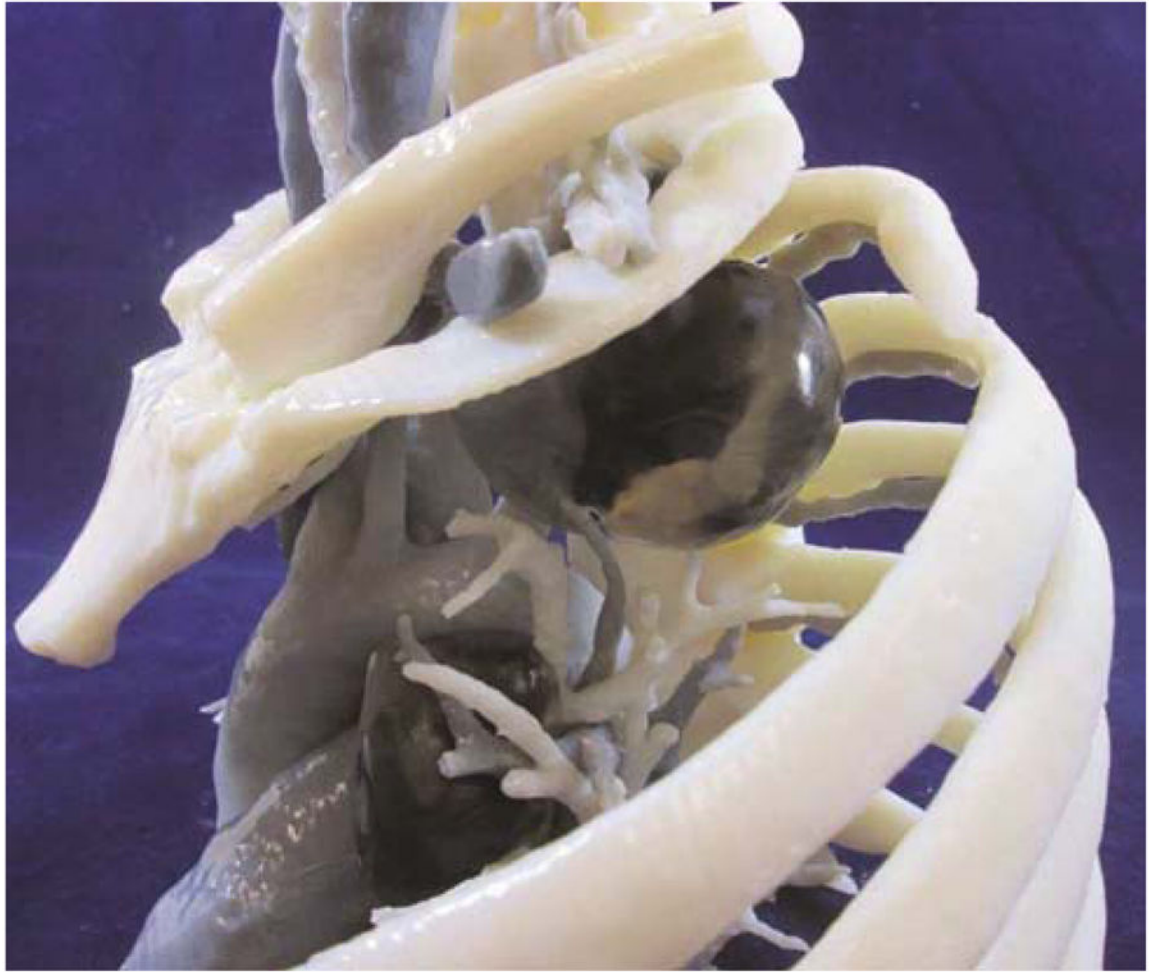


Figure 3. Anterior view of 5-dimensional model demonstrating pre-and post-treatment superior sulcus lung cancer and level 5 lymph nodes with clear representation of relationship of the tumor to surrounding structures (a). Lateral view with second rib removed for ease of viewing. Note the difference in size of tumor post-treatment (b).

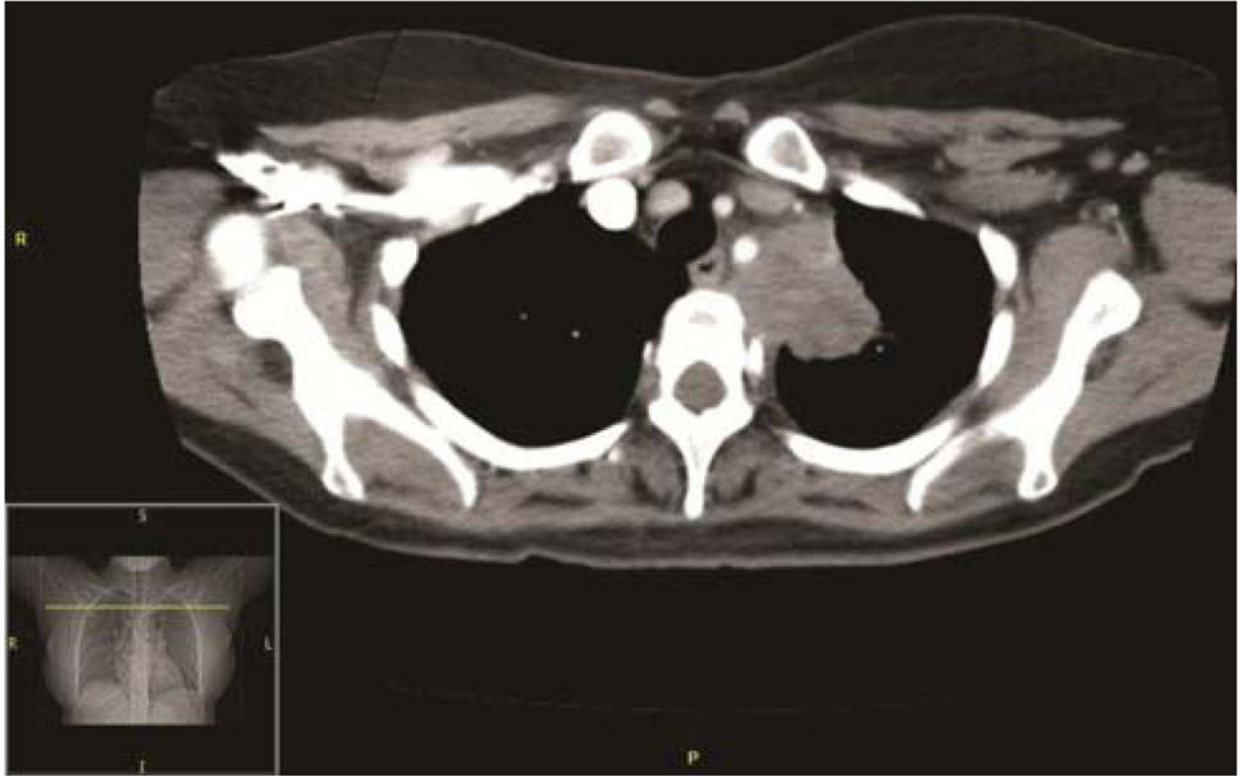


Figure 4.

The pre-treatment CT scan, demonstrating a superior sulcus lung tumor (4a) seen invading the mediastinum, abutting T2, the 1st and 2nd rib without evidence of destruction. The left subclavian artery is encased and displaced at and just distal to the origin of the vertebral artery. The post-treatment CT scan demonstrates superior sulcus tumor invading the mediastinum and abutting T2–T3. The mass has decreased in size (4b) and degree of encasement and displacement of the left subclavian artery is also reduced.

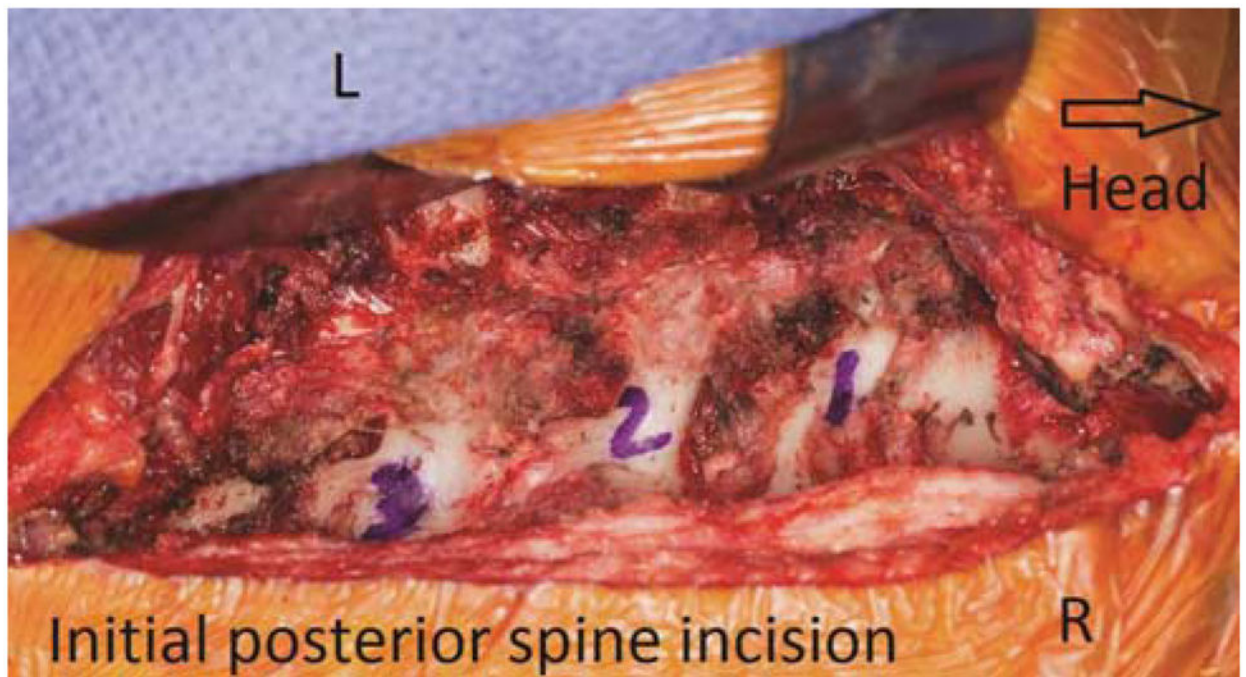


Figure 5. Posterior approach for division of the lateral aspect of the vertebral bodies, transections of the nerve roots, and separation of the posterior elements of the tumor. Orientation markers include L(left) and R(right).

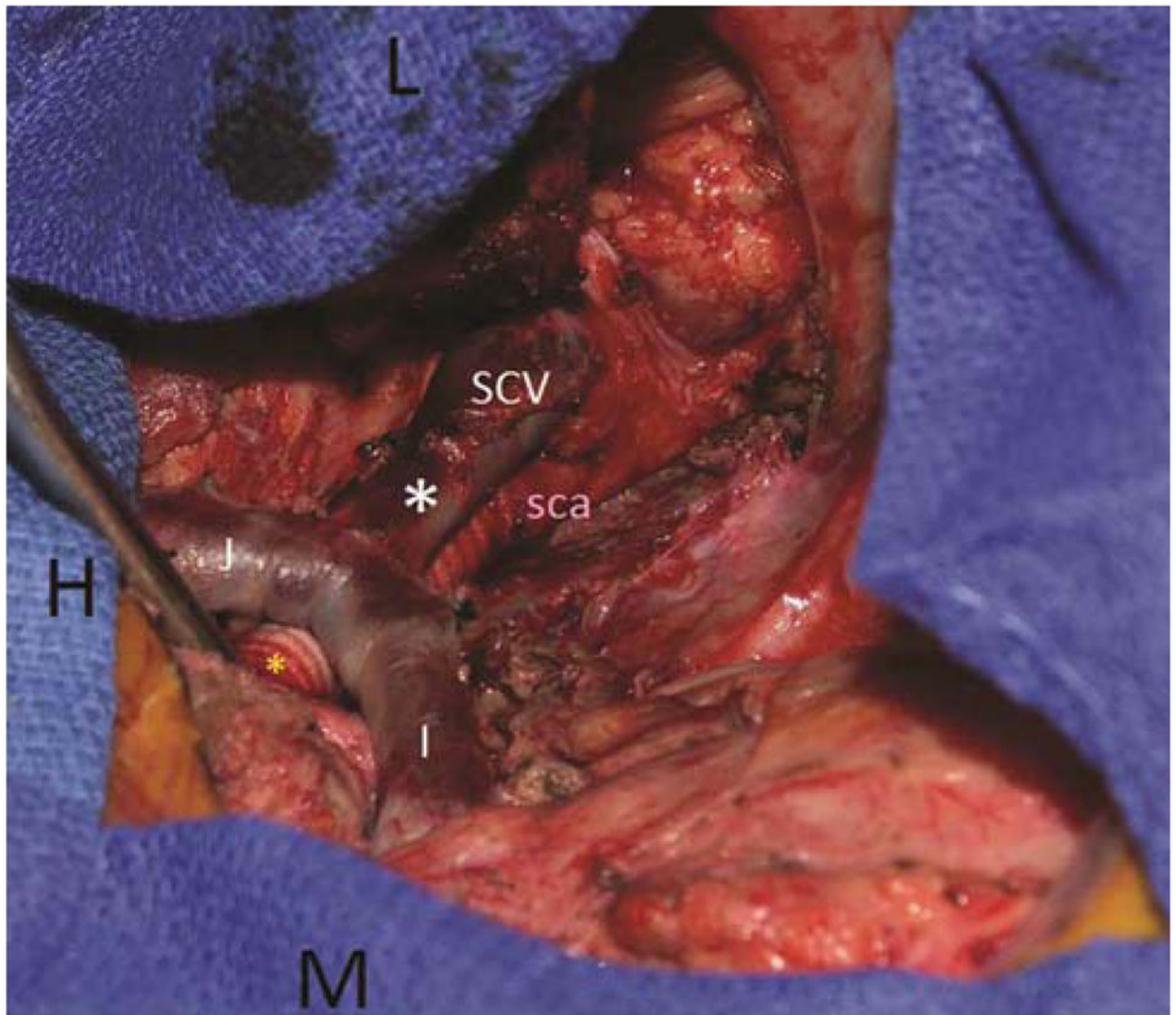


Figure 6. Second stage of the procedure was performed via a trap door anterior approach (head (H) to the left side of the photograph). The left lung is retracted laterally. The mediastinal structures were skeletonized, the thoracic duct was ligated, and the phrenic and vagus nerves were carefully preserved. The innominate (I) and tributaries were dissected, along with the underlying left carotid artery and proximal left subclavian artery (ligated the thyrocervical trunk and vertebral artery). A carotid subclavian bypass (yellow*) was performed with an 8 mm Hemagard Dacron graft. The re-implantation of the subclavian vein (SCV) is identified by the white*. The subclavian artery (sca) can be seen posterior to the vein as it is attached to the carotid-subclavian bypass. The markers include L(left & lateral) and M(medial).

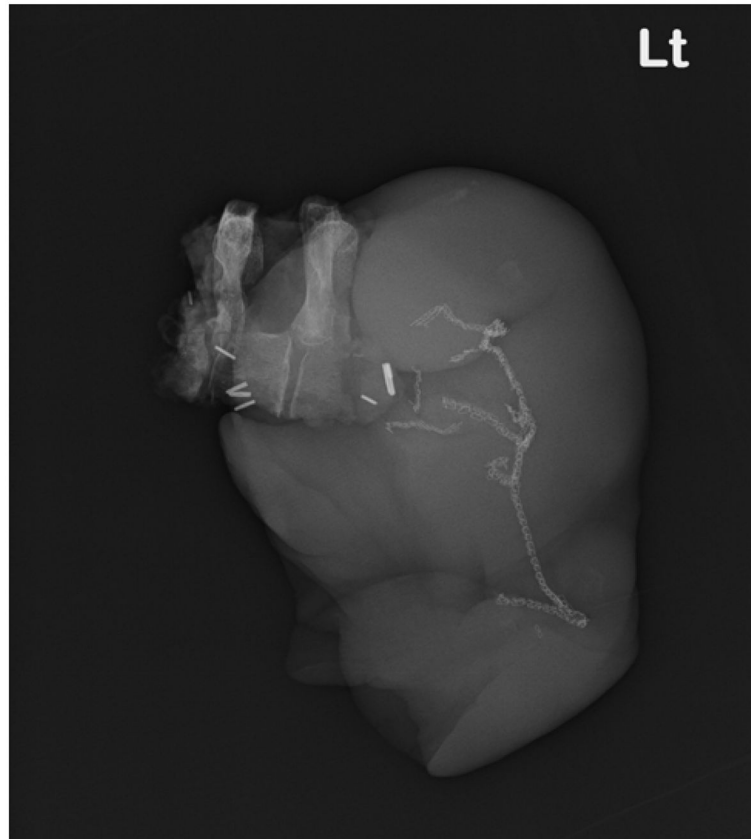


Figure 7.
The en bloc resection of the tumor with the left upper lobe of the lung is seen by radiograph.